

## **FLUID PROPULSION BY CILIA IN A SHEAR-THINNING FLUID**

**Michiel Baltussen<sup>1</sup>, Patrick Anderson\*<sup>1</sup>, Jaap den Toonder<sup>1,2</sup>**

<sup>1</sup>Eindhoven University of Technology, Materials Technology, Eindhoven, The Netherlands  
m.g.h.m.baltussen@tue.nl, p.d.anderson@tue.nl

<sup>2</sup>Philips Applied Technologies, Eindhoven, The Netherlands  
jaap.den.toonder@philips.com

### **KEY WORDS**

artificial cilia, human whole saliva, Non-Newtonian fluid flow, saliva rheology

### **ABSTRACT**

*Fluid propulsion by natural cilia is governed by their asymmetric motion. For artificial cilia driven by an external force, this asymmetry comes from the shape of the applied force and the initial shape of the cilium. For shear-thinning liquids such as saliva, which are deformation rate dependent, the motion can also become asymmetric due to different time-scales of the forward and the backward stroke. Using numerical simulations, we show that the time-scales can be controlled by the applied force amplitude. The model we use to describe the saliva behavior is based on rheological measurements we have performed on human whole saliva. We observe three times higher flow rates for saliva than for a Newtonian liquid with the same actuation and comparable cilia deflection. The dynamics of the cilium are also different.*

### **1. INTRODUCTION**

Fluid transport in systems with small dimensions is generally governed by viscous forces. Therefore many propulsion mechanisms we are used to in our daily life cannot be applied at small scales since they rely on inertial forces instead of viscous forces. Nature has found several mechanisms for transporting fluid at the sub millimeter length-scale, one of them being cilia which are small moving hairs. The cilia move in a cyclic manner and the path followed during the cycle determines the propulsion. If the path followed is symmetric, no net fluid flow is generated; if on the other hand the path is asymmetric, a net fluid flow results, since more material is transported in one direction than in the other. Since fluid transport by natural cilia is quite effective, many research groups mimic nature and build artificial cilia [1-5]. The main application of these artificial cilia is fluid transport in lab-on-chip devices for clinical diagnostics.

The artificial cilia are actuated by a magnetic force which governs the motion of the cilia, in combination with its initial shape. Since asymmetry of the motion of the cilia is the objective, this force is tailored in such a way that the cilia move asymmetrically. Many different approaches have been introduced to fabricate magnetic artificial cilia among which are chains of self assembled magnetic beads [6], connected beads [2], magnetic rods [4,7] and polymer flaps filled with magnetic particles [3,8].

Up to now most experimental and modeling research on ciliary flow has been using Newtonian liquids such as water or oil. A large group of fluids relevant for lab-in-chip devices, such as saliva and mucus but also synthetic polymer solutions, do not behave Newtonian because their viscosity is shear rate dependent or viscoelastic. The fluid flow of such non-Newtonian liquids induced by cilia may be fundamentally different from that in a Newtonian liquid and could even result in an enhanced net flow, since the non-constant viscosity can lead to different dynamics of the system.

The objective of this work is to study cilia dynamics and their induced flow in a non-Newtonian liquid using numerical simulations. The model liquid we will use is human whole saliva, which is a shear-thinning fluid.

---

\* Corresponding author

Since the amount of experimental rheological data present in literature is not large [9], we also present new rheological data.

The paper is structured as follows: in Section 2 the model of a cilium in a channel will be explained, Section 3 contains the methods used for determining the saliva viscosity, Section 4 presents the results from the experiments and the simulations and the main conclusions are stated in Section 6.

## 2. MODEL

We model a periodic array of cilia in a two-dimensional channel, see Fig. 1. Only one cilium is modeled and periodic boundary conditions are applied for the velocity. The cilium is fixed at the bottom of the channel. Both the fluid and the cilium are inertialess, incompressible and are modeled as a continuum. Initially the cilium stands straight on the lower wall.

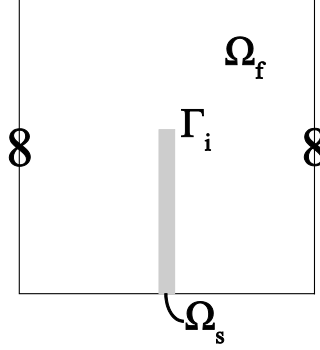


**Figure 1:** The modeled periodic domain with a single cilium. The fluid domain ( $\Omega_f$ ), grey solid domain ( $\Omega_s$ ) and the cilium boundary ( $\Gamma_i$ ) are indicated in the figure. The cilium has length  $L$  and thickness  $t$ , the domain is square and has dimensions  $(2L \times 2L)$ .

The cilium is modeled as a neo-Hookean solid, the fluid either as a Newtonian liquid or as a shear-thinning liquid. This leads to the following equations of motion for the cilium and surrounding fluid:

$$\nabla \cdot \boldsymbol{\sigma}_s = \mathbf{f}_s \quad \text{in } \Omega_s \quad (1)$$

$$\det(\mathbf{F}) - 1 = 0 \quad \text{in } \Omega_s \quad (2)$$

$$\nabla \cdot \boldsymbol{\sigma}_f = \mathbf{0} \quad \text{in } \Omega_f \quad (3)$$

$$\nabla \cdot \mathbf{u} = 0 \quad \text{in } \Omega_f \quad (4)$$

$$\mathbf{u} - \dot{\mathbf{d}} = \mathbf{0} \quad \text{on } \Gamma_i \quad (5)$$

$$\mathbf{n} \cdot \boldsymbol{\sigma}_s - \mathbf{n} \cdot \boldsymbol{\sigma}_f = \mathbf{0} \quad \text{on } \Gamma_i \quad (6)$$

where  $\boldsymbol{\sigma}_s$  is the Cauchy stress in the solid,  $\mathbf{f}_s$  is the actuation force density applied on the cilium,  $\det(\mathbf{F})$  is the determinant of the deformation gradient tensor  $\mathbf{F} = \nabla \mathbf{d}^T$ ,  $\boldsymbol{\sigma}_f$  is the Cauchy stress in the fluid,  $\mathbf{u}$  is the fluid velocity, and  $\dot{\mathbf{d}}$  is the displacement rate or solid velocity. The solid stress is given by  $\boldsymbol{\sigma}_s = G(\mathbf{B} - \mathbf{I}) - p_s \mathbf{I}$ , where  $G$  is the modulus of the solid,  $\mathbf{B} = \mathbf{F} \cdot \mathbf{F}^T$  is the Finger tensor,  $\mathbf{I}$  is the unit tensor, and  $p_s$  is the solid pressure. The fluid stress is given by  $\boldsymbol{\sigma}_f = 2\eta \mathbf{D} - p_f \mathbf{I}$ , where  $\eta$  is the viscosity which reads for a shear-thinning fluid:

$$\eta(\dot{\gamma}) = \eta_\infty + \frac{\eta_0 - \eta_\infty}{(1 + (\lambda \dot{\gamma})^2)^{(n-1)/2}} \quad (7)$$

where  $\dot{\gamma}$  is the shear rate,  $\eta_\infty$  is the viscosity at infinitely high shear rate,  $\eta_0$  the viscosity at zero shear rate,  $\lambda$  the time-scale at which the viscosity becomes rate dependent, and  $n$  the parameter giving the slope of the shear thinning region. The case  $n = 1$  represents a Newtonian fluid with  $\eta = \eta_0$ . The fluid stress is also a function of  $\mathbf{D} = \frac{1}{2}(\mathbf{L} + \mathbf{L}^T)$  which is the rate of deformation tensor with  $\mathbf{L} = \nabla \mathbf{u}^T$ , and  $p_f$  the fluid pressure.

The actuation force will only be applied in the horizontal direction.

The two-dimensional modeling is only valid if the channel and cilium width are much larger than the channel height and cilium length. Although this is usually not the case for a single cilium, it is true for a collection of cilia moving together in a wide channel. Obviously three dimensional actuation and motion of the cilia is also not possible, hence the results shown in this study cannot be compared with experiments involving three-dimensional motion. A 3D model requires significantly more computational effort compared to a 2D

model and since we are more interested in the fundamental differences between the two constitutive relations than in a comparison between simulations and experiments, we perform 2D simulations.

## 2.1 Scaling analysis

Scaling the governing equations gives relevant information about the expected velocity, displacement and time-scale in the system. By introducing a characteristic velocity  $U$ , displacement  $D$ , gradient  $\frac{1}{L}$ , time-scale  $t_{\text{ref}}$ , and actuation force per cilium volume  $f_0$ , the following non-dimensional groups appear:

$$R_1 = \frac{GD^2}{f_0 L^3}, \quad (8)$$

$$R_2 = \frac{U t_{\text{ref}}}{D}, \quad (9)$$

$$R_3 = \frac{GD^2}{\eta UL}. \quad (10)$$

Since the typical velocity, displacement and time-scale do not follow from essential boundary conditions, they are part of the problem, and the non-dimensional groups above must all be unity. This leads to the following expressions for  $D$ ,  $U$ ,  $t_{\text{ref}}$ :

$$D \propto \sqrt{\frac{f_0 L}{G}} L, \quad (11)$$

$$U \propto \frac{f_0 L^2}{\eta}, \quad (12)$$

$$t_{\text{ref}} \propto \frac{\eta}{G} \frac{1}{\sqrt{\frac{f_0 L}{G}}}. \quad (13)$$

From equations (11)-(13) it is clear that the characteristic parameters of the system depend on the material properties and the geometry, and also on the applied force. For a shear-thinning fluid, in contrast to a Newtonian fluid, also the time-scale at which the force is applied determines the characteristic parameters, in particular the characteristic velocity  $U$  and time-scale  $t_{\text{ref}}$ . The reason is that the viscosity appearing in equations (12) and (13) is then not constant but depends on the shear rate, and hence on the loading rate. In that case the characteristic velocity and time-scale can only be computed after the characteristic viscosity is known. If we define a characteristic shear-rate by  $\dot{\gamma} = \frac{U}{L} = \frac{f_0 L}{\eta(\dot{\gamma})}$ , then we obtain a characteristic shear stress of  $\tau_{xy} = \eta(\dot{\gamma})\dot{\gamma} = f_0 L$ . The characteristic shear-rate and viscosity at this shear stress can now be found in Figure 2, where a typical viscosity and corresponding shear stress profile are given for a shear-thinning fluid.

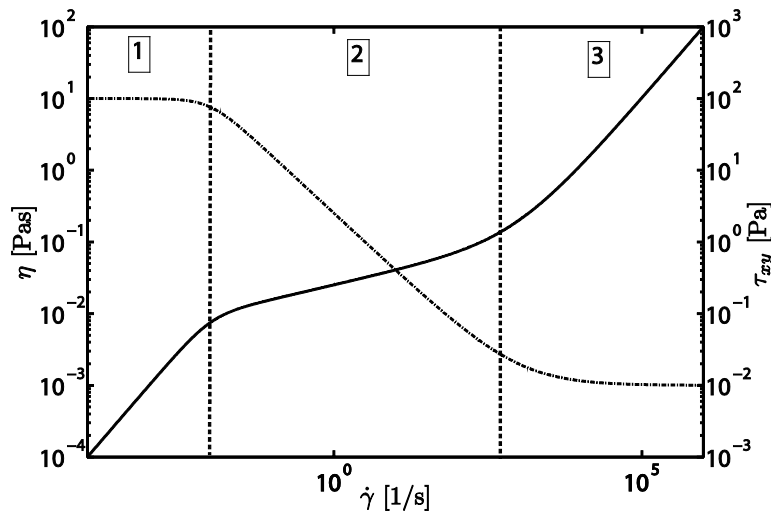


**Figure 2:** The viscosity (dashed line, left axis), as shear stress (solid line, right axis) for a shear-thinning fluid. Three regions are present: (1) Newtonian low shear-rate plateau, (2) shear-thinning region and (3) high shear-rate plateau.

Although it is important to get estimates of the characteristic displacement, velocity and time scale, it is much more interesting to see the influence of changes of these variables due to the changes in  $f_0$  because this

is the parameter that can be controlled in practice. In shear-thinning fluids, three regions can be distinguished (see Figure 2): region 1 where  $\tau_{xy}$  and  $\dot{\gamma}$  are low and  $\eta$  is high and independent of  $\dot{\gamma}$ , region 2, where  $\eta$  rapidly decreases with increasing shear-rate, this is the shear-thinning region, and region 3 where  $\tau_{xy}$  is large and the viscosity independent of  $\dot{\gamma}$ , but lower than in region 1. A change of  $f_0$  within regions 1 and 3 will only result in a small change of characteristic time-scale, velocity and displacement as given by equations (10)-(12); the viscosity remains the same however, hence this situation is the same as for a Newtonian fluid. In the second region a change in  $f_0$  leads to large changes in  $\eta$  and therefore the characteristic velocity and time scale will change too as can be seen in equations (12) and (13), far more than in the first and third region.

We anticipate that, for the effect of the non-Newtonian behavior to be largest, possibly resulting in enhanced net flow, the dynamic contrast between the forward and the backward stroke of the cilia should be large, and therefore different forces should be applied shifting back and forth between different positions in region 2 of Figure 2. To study this, we propose the following actuation scheme; apply a large actuation force  $f_1$  for a time  $\Delta t_1$  as forward stroke and a smaller force  $f_2$  for  $\Delta t_2$  as a backward stroke. Both forces only act in horizontal direction, and are related as follows:  $\frac{f_1}{f_2} = \frac{\Delta t_2}{\Delta t_1}$ . We therefore have three free parameters:  $f_1$ ,  $f_2$  and  $\Delta t_1$ . Since the characteristic time-scale is  $t_{\text{ref}}$ , and the typical time-scale of applying the force are  $\Delta t_1$  and  $\Delta t_2$ , two new dimensionless groups appear:

$$R_4 = \frac{t_{\text{ref}}}{\Delta t_1} \quad (14)$$

$$R_5 = \frac{t_{\text{ref}}}{\Delta t_2} \quad (15)$$

which give the ratios of the characteristic time-scale of the system to the time-scales of the applied force. If both are smaller than unity the cilium moves to its steady state position and remains there for the remainder of the stroke. If  $R_4$  or  $R_5$  are larger than unity the steady state position is not reached before the end of the applied force. See Figure 3 for a schematic view of the two situations.

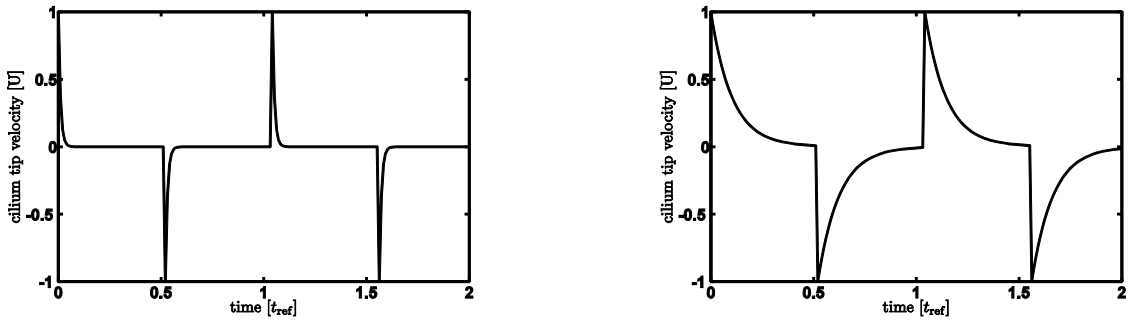


**Figure 3:** Cilium tip velocity as function of time for  $R_4 < 1, R_5 < 1$  (left) and  $R_4 > 1, R_5 > 1$  (right).

From the scaling analysis it follows that for a given system, the actuation force governs the time scale of movement, *i.e.* it controls the dynamics of the system. In particular, if the two non-dimensional numbers  $R_4$  and  $R_5$  are different, the dynamical behavior of the system is different between the forward and the backward strokes, which can lead to asymmetric cilia motion. This is true for a Newtonian as well as for a shear-thinning fluid. However for a shear-thinning fluid this difference can be much more pronounced since the characteristic time scale  $t_{\text{ref}}$  itself depends on the time scale of the applied force through its viscosity dependence, as explained above. The relation between  $R_4$  and  $R_5$  is as follows:

$$R_4 = \frac{\eta_1}{\eta_2} \sqrt{\frac{f_1}{f_2}} R_5 \quad (16)$$

where  $\eta_1$  and  $\eta_2$  are the typical viscosities in forward and backward stroke respectively. So the force ratio has a smaller influence on the difference in dynamics during forward and backward stroke than the viscosity ratio. Hence even for small force ratios large differences in dynamics can be apparent when the fluid is shear-thinning.

## 2.2 Computational model

The set of governing equations (1-6) is solved with the extended finite element method. The interface conditions (5-6) are imposed by a new interface coupling scheme recently developed by the authors [10]. This scheme is based on the embedded Dirichlet boundary condition method by Gerstenberger and Wall [11]. We use a bi-quadratic interpolation for the velocity and displacement and bi-linear interpolation for the fluid and solid pressure.

### 3. MATERIALS AND METHODS

The rheology of human whole saliva (WHS) is tested using an ARES 902-30004 rheometer of Rheometric Scientific. A plate-plate setup (50 mm diameter plates) was used. Of five test subjects saliva was collected by letting them drool into a plastic cup. The drooling prevented much of the air bubbles, which are usually present in saliva and hence homogeneous samples were obtained. The donors were instructed not to eat or drink anything other than water for one and a half hours before the test. Directly after donation, 2-3 ml of saliva was pipetted in between the plates of the rheometer. Then a series of steady-state shear tests were performed where the steady-state viscosity was measured after 50s of shearing at shear-rates of 1 up to 500 1/s. The series were performed four times, where the results from the first set were disregarded, since they always showed lower and non-reproducible viscosities. The most likely reason for this behavior are air bubbles, which are broken up at the high shear-rates of the first series. The results of the remaining three series were reproducible. Initial tests in which the viscosity was recorded from the commence of shearing showed that it took 50s to reach steady state, hence the steady state viscosity was recorded only after 50s.

### 4. RESULTS

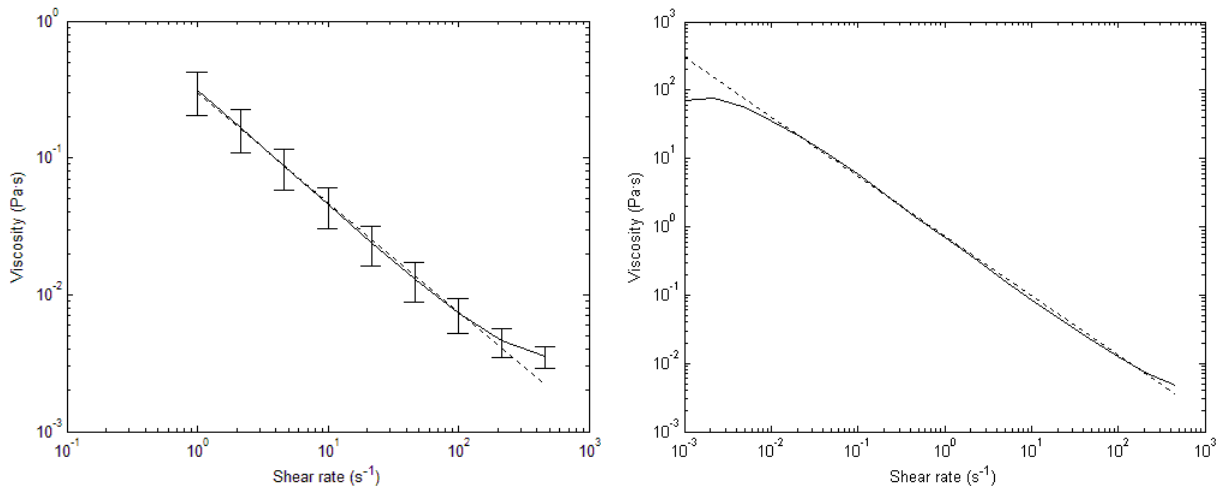


**Figure 4:** Left: The measured saliva viscosity for all test subjects, showing clear shear thinning. The error bars indicate the standard deviation. Right: A single measurement of saliva of only one test subject over a wider range, showing a low shear-rate plateau of 70 Pa·s. Measurements at higher shear rates were not possible due to fluid inertial effects.

The saliva rheology data is shown in Figure 4 on the left. The error bars indicate the standard deviation of all measurements and test subjects and is due to differences between the subjects, not between different measurements of the same sample. This shows that the test method used is reproducible. It is also clear that saliva is extremely shear thinning, since the viscosity declines rapidly over this range of shear rates, whilst no zero-shear rate plateau and infinite shear rate plateau is found. A wider range of shear rates has been used for only one test person and is shown in Figure 4 on the right. It shows the remarkably high zero shear rate plateau of 70 Pa·s. It is expected that the viscosity remains constant at 1 mPa·s at higher shear rates, which is the viscosity of water. A fit of Equation (7) to this measurement yields  $n = 0.2$ ,  $\eta_0 = 70 \text{ Pa} \cdot \text{s}$ ,  $\eta_\infty = 1 \text{ mPa} \cdot \text{s}$ ,  $\lambda = 100\text{s}$ .

We have carried out simulations for a Newtonian liquid with  $\eta = 0.1 \text{ Pa} \cdot \text{s}$  and a shear thinning liquid with the parameters above. The domain is  $1 \text{ mm} \times 1 \text{ mm}$ , the cilium is  $L \times t = 0.5 \text{ mm} \times 10 \mu\text{m}$  and the actuation force is varied in order to investigate its influence. Simulations have been performed for 20 cycles, in order to exclude transient effects.

Simulations have been performed for  $\Delta t_1 = 0.02$  s,  $\Delta t_2 = 0.04$  s and for two different actuation forces  $f_1 = 2 \cdot 10^5$  N/m<sup>3</sup> and  $f_1 = 4 \cdot 10^5$  N/m<sup>3</sup>. This results in  $f_2 = 1 \cdot 10^5$  N/m<sup>3</sup> and  $f_2 = 2 \cdot 10^5$  N/m<sup>3</sup>.

The cilium trajectories for both the Newtonian and shear-thinning fluid and an actuation force of  $f_1 = 4 \cdot 10^5$  N/m<sup>3</sup> are shown in Figure 5. The red positions are obtained during forward motion, the blue positions during backward motion. While the path of the cilium is more or less symmetric around the initial configuration for the Newtonian fluid, the path in the shear-thinning fluid is tilted in the forward stroke direction. This is a direct consequence of the different viscosities and time-scales during the forward and backward stroke. Since the forward stroke involves a higher force, the time-scale is shorter and hence there will be more deflection. During the backward stroke the force is lower and the time-scale is larger. For the Newtonian fluid  $R_4 = \sqrt{2}R_5$ , for this actuation scheme, so the dynamics are different during forward and backward stroke. A similar analysis for the shear-thinning fluid requires information on the actual viscosities, which will be shown in the next paragraph.



**Figure 5:** The forward (blue) and backward (red) stroke of a cilium in a Newtonian fluid (left) and the shear-thinning fluid (right). Both have the same actuation cycle with  $f_1 = 4 \cdot 10^5$  N/m<sup>3</sup>.

A typical viscosity profile at the start of forward and backward actuation is shown in Figure 6, from which it is clear that the lowest viscosity found in forward stroke is about 10 times lower than the viscosity found in the backward stroke. This leads to  $R_4 = 0.1 \sqrt{2}R_5$ , so a ten times smaller ratio than for the Newtonian case. It is also clear that the viscosity itself is not constant over the entire domain, thus leading to different flow profiles further away from the cilium. This has also been observed by Smith *et al.* [12] in a Maxwell fluid, where particle motion was different for a Newtonian liquid than for the Maxwell fluid.

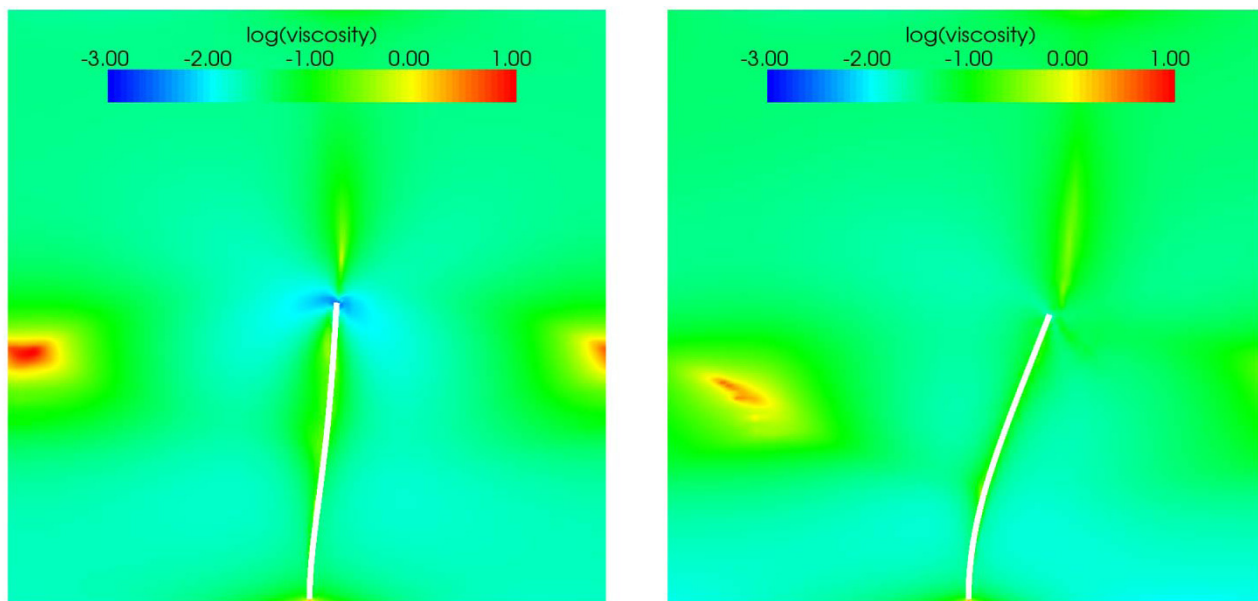


**Figure 6:** The decadic logarithm of the viscosity at the beginning of forward stroke of the 11<sup>th</sup> cycle (left) and at the beginning of the backward stroke of the same cycle (right).

The net flow produced during one actuation cycle is computed at the 11<sup>th</sup> cycle. The path followed by the cilium is constant for each cycle by then, so no transient effects are observed anymore. The channel width is taken 1 mm, yielding a square channel cross-section. In addition to the net flow per cycle the net flow per

minute is given. In order to quantify the efficiency, the ratio of the net flow per cycle and the total flow in forward and backward direction is taken as the efficiency. For the studied actuation parameters this yields the following values (Table 1):

Fluid model	Body force, $f_1$ , (N/m <sup>3</sup> )	Net flow ( $\mu\text{l}/\text{cycle}$ )	Net flow ( $\mu\text{l}/\text{min}$ )	Efficiency (%)
Newtonian	$2 \cdot 10^5$	$3.3 \cdot 10^{-4}$	0.33	1.3
Newtonian	$4 \cdot 10^5$	$6.0 \cdot 10^{-4}$	0.60	1.2
Shear-thinning	$2 \cdot 10^5$	$2.6 \cdot 10^{-4}$	0.26	2.4
Shear-thinning	$4 \cdot 10^5$	$1.9 \cdot 10^{-3}$	1.87	4.0

**Table 1:** Net flow and efficiency results for different body forces and constitutive models.

So flow is generated in all cases, but the flow of a shear-thinning fluid with the same actuation is lower for the low force and three times higher for the higher force. The efficiency is low in both cases, but for the Newtonian fluid it is at least 50% lower than for the shear-thinning fluid.

## 5. ACKNOWLEDGMENTS

This work is a part of the 6th Framework European project ‘Artic’, under contract STRP 033274. The authors would like to thank Rene Thijssen for performing the saliva rheological experiments.

## 6. CONCLUSION

The motion of a single cilium in a periodic array has been modeled, both within a Newtonian and a shear-thinning fluid. Scaling analysis shows that the characteristic displacements, velocities and time-scales of the system are determined by the solid modulus, cilium length, fluid viscosity and applied force only. Hence for a system with a given geometry and modulus, the applied force is the only control parameter. The dynamical response of the cilium to the applied force is determined by the ratio of the characteristic time-scale of the system itself to the time-scale of applying the load both for Newtonian and shear-thinning fluids. Hence, applying different forces and loading rates during the forward and the backward stroke can lead to asymmetric motion of the cilium resulting in a net induced flow. This effect can be much larger for shear-thinning fluids, and non-Newtonian fluids in general, than for Newtonian fluids due to the shear-rate dependency of viscosity of the former, causing a different viscosity and hence different characteristic time scale between the two strokes. We found that, for a particular design of the system, this difference in dynamical behavior led to three times higher flow rates and a doubling of the efficiency for saliva than for a Newtonian liquid with the same actuation and comparable cilia deflection.

## REFERENCES AND CITATIONS

- [1] Toonder, J.M.J. den, Bos, F.M., Broer, D.J., Filippini, L., Gillies, M., Goede, J. de, Mol, G.N., Talen, W., Wilderbeek, J.T.A., Khataavkar, V., & Anderson, P.D. (2008), Artificial cilia for active micro-fluidic mixing, *Lab Chip*, **8**, 533-541.
- [2] Gauger, E.M., Downton, M.T., & Stark, H. (2009), Fluid transport at low Reynolds number with magnetically actuated artificial cilia. *Eur. Phys. J. E.*, **28**, 231-242.
- [3] Khaderi, S. N, Baltussen, M, Anderson, P. D, Ioan, D, den Toonder, J. M. J, & Onck, P. R. (2009), Nature-inspired microuidic propulsion using magnetic actuation, *Physical Review E*, **79**, 46304.
- [4] Evans, B.A., Shields, A.R., Lloyd Carroll, R., Washburn, S., Falvo, M.R., & Superfine, R. (2007), Magnetically actuated nanorod arrays as biomimetic cilia, *nanoletters*, **7**, 1428-1434
- [5] Alexeev, A, Yeomans, J. M, & Balazs, A. C. (2008), Designing synthetic, pumping cilia that switch the flow direction in microchannels, *Langmuir*, **24**, 12102-6.
- [6] Vilfan, M., Potocnik, A., Kavcic, B., Osterman, N., Poberaj, I., Vilfan & A., Babic, D. (2010), Self-assembled artificial cilia, *PNAS*, **107**, 1844-1847.
- [7] Shields, A.R., Fiser, L., Evans, B.A., Falvo, M.R., Washburn, S. & Superfine, R. (2010), Biomimetic cilia arrays generate simultaneous pumping and mixing regimes, *PNAS*, **107**, 15670-15675.
- [8] Fahrni, F., Prins, M.W.J. & IJzendoorn, L.J. (2009), Micro-fluidics actuation using magnetic artificial cilia, *Lab Chip*, **9**, 3413-3421.
- [9] Stokes, J.R., & Davies, G.A. (2007). Viscoelasticity of human whole saliva collected after acid and mechanical stimulation, *Biorheology*, **44**, 141-160.

- [10] Baltussen, M.G.H.M., Choi, Y.J., Hulsen, M.A., Anderson, P.D. An embedded Dirichlet condition for non-Newtonian fluids, in preparation.
- [11] Gerstenberger, A., & Wall, W.A. (2010). An embedded Dirichlet formulation for 3D continua, *Int. J. Numer. Meth. Engng*, **82**, 537-563.
- [12] Smith, D.J., Gaffney, E.A., & Blake, J.R. (2009). Mathematical modeling of cilia-driven transport of biological fluids. *Proc. R. Soc. A.*, **465**, 2417-2439.